

Synthesis, Purification, and Structural Characterization of the Dimethyldiselenoarsinate Anion

Jürgen Gailer,^{*,†} Graham N. George,[‡] Hugh H. Harris,[‡] Ingrid J. Pickering,[‡] Roger C. Prince,[§] Arpad Somogyi,^{||} Gavin A. Buttigieg,^{||} Richard S. Glass,^{||} and M. Bonner Denton^{||}

Institute for Ecological Chemistry, GSF—National Research Center for Environment and Health, Ingolstädter Landstrasse 1, D-85764 Neuherberg, Germany, Stanford Linear Accelerator Center, Stanford Synchrotron Radiation Laboratory, MS 69, 2575 Sand Hill Road, Menlo Park, California 94025, ExxonMobil Research and Engineering Company, Route 22 East, Annandale, New Jersey 08801, and Department of Chemistry, The University of Arizona, Tucson, Arizona 85721

Received December 27, 2001

A novel arsenic–selenium solution species was synthesized by reacting equimolar sodium selenite and sodium dimethylarsinate with 10 mol equiv of glutathione (pH 7.5) in aqueous solution. The solution species showed a single ⁷⁷Se NMR resonance at 112.8 ppm. Size-exclusion chromatography (SEC) using an inductively coupled plasma atomic emission spectrometer (ICP-AES) as the simultaneous arsenic-, selenium-, sulfur-, and carbon-specific detector revealed an arsenic–selenium moiety with an As:Se molar ratio of 1:2. Electrospray ionization mass spectrometry (ESI-MS) of the chromatographically purified compound showed a molecular mass peak at *m/z* 263 in the negative ion mode. Fragmentation of the parent ion (ESI-MS-MS) produced (CH₃)₂As[−] and Se₂[−] fragments. Arsenic and selenium extended X-ray absorption fine structure spectroscopy (EXAFS) of the purified species revealed two As–C interactions at 1.943 Å and two As–Se interactions at 2.279 Å. On the basis of these results this novel solution species is identified as the dimethyldiselenoarsinate anion.

Introduction

Arsenic and selenium are widely distributed in a variety of mineral deposits, particularly those containing sulfides and sulfo salts.^{1,2} Weathering of these mineral deposits mobilizes the water-soluble inorganic oxo anions arsenite, arsenate, selenite, and selenate to the hydrosphere.^{1–4} In addition, human activities also emit substantial amounts of inorganic arsenic and selenium to the environment.^{4,5} Among the environmentally abundant arsenic and selenium compounds, arsenite and selenite are most acutely toxic and teratogenic.⁶

Human metabolism of arsenite involves the urinary excretion of numerous methylated arsenic compounds (together with unchanged arsenite and arsenate).^{7,8} These methylation reactions are carried out by arsenite methyltransferase and monomethylarsonic acid methyltransferase which have been partially purified from rabbit liver cytosol.⁹ Likewise, when rats were exposed to selenite, the methylated selenium species (CH₃)₃Se⁺ and CH₃SeH were identified in the urine (together with inorganic selenium)¹⁰ and (CH₃)₂Se was exhaled.¹¹ As for the biomethylation of arsenite, the biotransformations of selenite are enzymatically mediated.¹² In contrast to inorganic arsenic, however, inorganic selenium is also incorporated into numerous selenoproteins.¹³

* Corresponding author: Telephone: 089-3187-2430. Fax: 089-3187-3348. E-mail: gailer@gsf.de.

† GSF.

‡ Stanford Synchrotron Radiation Laboratory.

§ ExxonMobil Research and Engineering Company.

|| The University of Arizona.

- (1) Boyle, R. W.; Jonasson, I. R. *J. Geochem. Explor.* **1973**, *2*, 251–296.
- (2) Berrow, M. L.; Ure, A. M. *Occurrence and Distribution of Selenium*; Ichnat, M., Ed.; CRC Press: Boca Raton, FL, 1989; pp 213–242.
- (3) Conde, J. E.; Alaejos, M. S. *Chem. Rev.* **1997**, *97*, 1979–2003.
- (4) Brown, G. E., Jr.; Foster, A. L.; Ostergren, J. D. *Proc. Natl. Acad. Sci. U.S.A.* **1999**, *96*, 3388–3395.
- (5) Nriagu, J. O.; Pacyna, J. M. *Nature* **1988**, *333*, 134–139.

- (6) Keen, C. L. *Toxicology of Metals*; Chang, L. W., Ed.; CRC Lewis Publishers: Boca Raton, FL, 1996; pp 977–1001.
- (7) Braman, R. S.; Foreback, C. C. *Science* **1973**, *182*, 1247–1249.
- (8) Mandal, B. K.; Ogra, Y.; Suzuki, K. T. *Chem. Res. Toxicol.* **2001**, *14*, 371–378.
- (9) Zakharyan, R.; Wu, Y.; Bogdan, G. M.; Aposhian, H. V. *Chem. Res. Toxicol.* **1995**, *8*, 1029–1038.
- (10) Itoh, M.; Suzuki, K. T. *Arch. Toxicol.* **1997**, *71*, 461–466.
- (11) Ganther, H. E. *J. Am. Coll. Toxicol.* **1986**, *5*, 1–5.
- (12) Hsieh, H. S.; Ganther, H. E. *Biochim. Biophys. Acta* **1977**, *497*, 205–217.

In the late 1930s Moxon and co-workers discovered that the addition of arsenite to drinking water (5.0 mg of As/L) completely prevented the symptoms of selenium poisoning caused by either dietary selenite or the same concentration of selenium as seleniferous wheat (11.0 mg of Se/kg).^{14,15} This was the first experimental evidence suggesting that the metabolism of arsenite and selenite are linked. Subsequent studies revealed that arsenite greatly increased the biliary excretion of selenium (given as sodium selenite),¹⁶ and vice versa.¹⁷ The molecule that links the metabolism of arsenite with that of selenite was finally identified in rabbit bile as the seleno-bis (*S*-glutathionyl)arsinium ion, $[(\text{GS})_2\text{AsSe}]^-$.^{18–20}

It has not yet been shown whether environmental arsenic compounds other than arsenite also react with selenite and glutathione (GSH), thereby potentially affecting the metabolism and excretion of simultaneously ingested dietary selenium. One such environmentally abundant arsenic compound is dimethylarsinic acid, which occurs in fresh and saline waters,⁷ occurs in seafood,²¹ and is frequently used as an insecticide, pesticide, and herbicide (the sodium salt).^{22–24} Additionally, dimethylarsinic acid is one of the major urinary metabolites following the ingestion of inorganic arsenic by mammals.^{8,9} To investigate if dimethylarsinic acid will react with selenite and reduced glutathione (GSH), an aqueous solution containing equimolar sodium selenite and sodium dimethylarsinate was reacted with excess GSH and the product was analyzed with a variety of chromatographic and spectroscopic techniques. These studies allowed the structural characterization of a novel arsenic–selenium solution species of potential physiological significance.

Experimental Section

Caution! *Inorganic selenium is teratogenic and inorganic arsenic compounds are highly toxic and are established human carcinogens. Ingestion of inorganic arsenic may cause cancer of the skin, urinary bladder, kidneys, lungs, and liver, as well as disorders of the circulatory and nervous systems.*

Chemicals. Sodium selenate (Na_2SeO_4), sodium selenite ($\text{Na}_2\text{SeO}_3 \cdot 5\text{H}_2\text{O}$), sodium arsenate heptahydrate ($\text{Na}_2\text{HAsO}_4 \cdot 7\text{H}_2\text{O}$), sodium dimethylarsinate $[(\text{CH}_3)_2\text{As}(\text{O})\text{ONa} \cdot 2.5\text{H}_2\text{O}]$, reduced glutathione (GSH), oxidized glutathione (GSSG), dipotassium hydrogen phos-

phate (K_2HPO_4), potassium dihydrogen phosphate (KH_2PO_4), potassium sulfate (K_2SO_4), and rat hemoglobin (twice crystallized) were purchased from Sigma and used without further purification. Aqueous solutions containing As:Se molar ratios of 1:1, 1:2, 1:3, and 2:1 were prepared by dissolving appropriate amounts of sodium arsenate and sodium selenite in distilled water.

Synthesis of Arsenic–Selenium Solution Species. Since preliminary experiments showed that at least 8 mol equiv of GSH are required to obtain a colorless reaction mixture with equimolar dimethylarsinic acid/selenite (less resulted in a brown precipitate), 10 mol equiv was used to protect a potentially formed oxygen sensitive arsenic–selenium species. A solution containing equimolar dimethylarsinate and selenite was prepared by dissolving $(\text{CH}_3)_2\text{As}(\text{O})\text{ONa} \cdot 2.5\text{H}_2\text{O}$ (213 mg, 1.038 mmol) and $\text{Na}_2\text{SeO}_3 \cdot 5\text{H}_2\text{O}$ (275 mg, 1.045 mmol) to 1.0 cm^3 using distilled water (solution A). Then GSH (254 mg, 0.827 mmol) was dissolved in distilled water, the pH was adjusted to 7.5, and the solution was diluted to 1.0 cm^3 . After incubation of this solution for 20 min at 37 °C, an aliquot of solution A (80 μL) was added. A red-brown precipitate (likely elemental selenium) formed and dissolved upon mixing to yield a colorless and clear solution of pH 8.7 with a characteristic garlic-like smell. Addition of HCl to this solution produced a brown precipitate.

⁷⁷Se NMR. The arsenic–selenium solution species was prepared as described above using D_2O . The 95.344 MHz ⁷⁷Se NMR spectrum was acquired without spinning at 25 °C on a Bruker DRX-500 spectrometer using a 5 mm o.d. glass tube in a broad-band direct probe with proton decoupling. The external standard was PhSeSePh (1.0 M in CHCl_3 , fused in a glass capillary and placed into the NMR tube), which provided a single selenium resonance at $\delta = 463$ ppm.²⁵ Using a 30° pulse (pulse width 5 μs) at a spectral width of 100,000 Hz and a relaxation delay of 2 s, 26 723 scans were accumulated.

Size-Exclusion Chromatography (SEC). A Beckman 110B solvent delivery module HPLC pump in conjunction with a Rheodyne six-port injection valve (200 μL loop) was used. A Pharmacia HR 10/30 column (1.0 cm i.d.) was packed with Sephadex G-10 (Amersham Pharmacia Biotech AB, Uppsala, Sweden). The mobile phase was prepared by mixing 0.05 mol dm^{-3} solutions of KH_2PO_4 and K_2HPO_4 to obtain a solution with pH 8.0. After equilibration (column height 29.4 cm), the column exit was connected to the Meinhard TR-30-K2 concentric nebulizer of the ICP-AES with polyethylene tubing. A flow rate of 1.0 $\text{cm}^3 \text{min}^{-1}$ was used throughout the study, and all chromatographic procedures were carried out at 25 °C. The column was size calibrated with rat hemoglobin [Fe-specific detection at 259.940 nm (order 130)], GSSG, GSH (S-specific detection), Na_2SO_4 [Na-specific detection at 330.237 nm (order 102)], sodium selenite and sodium arsenite (As- and Se-specific detection). The retention times were 8.7, 9.0, 11.6, 12.0, 13.4, and 21.5 min, respectively.

ICP-AES Detection. Simultaneous arsenic-, selenium-, sulfur-, and carbon-specific detection was achieved with a Thermo Jarrel Ash (Franklin, MA) IRIS HR radial view ICP-AES at 228.812, 206.279, 182.624, and 247.856 nm (order 147, 164, 184, and 136). Time-scan functions were carried out by Thermo-SPEC/CID software (version 2.2.1.c1; one atomic emission line was processed every 0.02 s). The nebulization gas flow was 2.0 $\text{dm}^3 \text{min}^{-1}$, the plasma forward power was 1150 W, and the CID temperature was maintained at –85 °C. To determine the recovery, column effluent was collected for 40 min (post injection), diluted to 50 cm^3 with mobile phase, and quantified against stock solutions of As, Se, and

- (13) Hawkes, W. C.; Wilhelmsen, E. C.; Tappel, A. L. *J. Inorg. Biochem.* **1985**, *23*, 77–92.
 (14) Moxon, A. L. *Science* **1938**, *88*, 81.
 (15) Dubois, K. P.; Moxon, A. L.; Olson, O. E. *J. Nutr.* **1940**, *19*, 477–482.
 (16) Levander, O. A.; Baumann, C. A. *Toxicol. Appl. Pharmacol.* **1966**, *9*, 106–115.
 (17) Levander, O. A.; Baumann, C. A. *Toxicol. Appl. Pharmacol.* **1966**, *9*, 98–105.
 (18) Gailer, J.; George, G. N.; Pickering, I. J.; Prince, R. C.; Ringwald, S. C.; Pemberton, J. E.; Glass, R. S.; Younis, H. S.; DeYoung, D. W.; Aposhian, H. V. *J. Am. Chem. Soc.* **2000**, *122*, 4637–4639.
 (19) Gailer, J.; Madden, S.; Burke, M. F.; Denton, M. B.; Aposhian, H. V. *Appl. Organomet. Chem.* **2000**, *14*, 355–363.
 (20) Gailer, J.; Madden, S.; Buttigieg, G. A.; Denton, M. B.; Younis, H. S. *Appl. Organomet. Chem.* **2002**, *16*, 72–75.
 (21) Benramdane, L.; Bressolle, F.; Vallon, J. J. *J. Chromatogr. Sci.* **1999**, *37*, 330–344.
 (22) Ishiguro, S. *Appl. Organomet. Chem.* **1992**, *6*, 323–331.
 (23) Males, R. G.; Nelson, J. C.; Phillips, P. S.; Cullen, W. R.; Herring, F. G. *Biophys. Chem.* **1998**, *70*, 75–85.
 (24) Spiewak, R. *Ann. Agric. Environ. Med.* **2001**, *8*, 1–5.

- (25) Duddeck, H. *Prog. NMR Spectrosc.* **1995**, *27*, 1–323.

S prepared in mobile phase. The recoveries of As, Se, and S were 83 ± 3 , 89 ± 5 , and $86 \pm 4\%$. As:Se intensity ratios of the arsenic- and selenium-containing peak (at the peak maximum) were compared with those of aqueous solutions with As:Se molar ratios of 1:1, 1:2, 1:3, and 2:1.

Electrospray Ionization Mass Spectrometry (ESI-MS). A Finnigan LCQ ion trap instrument was used to detect negatively charged ions in the solution. An aqueous solution of the sample (concentration $\approx 200 \mu\text{mol dm}^{-3}$) was introduced into the ESI source with a flow rate of $20 \mu\text{L min}^{-1}$. The needle voltage was 4.5 kV and the capillary voltage was 50 V.

X-ray Absorption Spectroscopy. X-ray absorption spectra were recorded on beamline 7-3 at the Stanford Synchrotron Radiation Laboratory with the SPEAR storage ring containing 50–100 mA at 3.0 GeV. A Si(220) double crystal monochromator with an upstream aperture of 1 mm was used, and no specular optics were present in the beamline. Harmonic rejection was accomplished by detuning one monochromator crystal by approximately 50%. X-ray absorption was monitored using N_2 -filled ionization chambers. The sample was maintained at a temperature of 10 K during data acquisition using an Oxford Instruments liquid helium cryostat. The spectrum of an elemental foil (α -As or hexagonal Se) was recorded simultaneously with each scan. X-ray energy calibration was by reference to the lowest energy K-edge inflection of the foil standard which was assumed to be 11 867.0 and 12 658.0 eV for As and Se, respectively. Data were collected using the program XAS•Collect,²⁶ and the extended X-ray absorption fine structure (EXAFS) spectra were analyzed with the EXAFSPAK program suite,²⁷ employing ab initio phase and amplitude functions calculated with the program FEFF (version 8.25).²⁸

Molecular Modeling. The optimized geometry for dimethyldiselenoarsinate $[(\text{CH}_3)_2\text{AsSe}_2]^-$ was determined using the program Dmol³ Materials Studio version 2.0.^{29,30} The Becke exchange³¹ and Perdew correlation³² functionals were used to calculate both the potential during the SCF and the energy. Double numerical basis sets included polarization functions for all atoms. Calculations were spin-unrestricted and effective core potentials were used in place of As and Se core orbitals ($n = 1, 2, \text{ and } 3$). No symmetry constraints were applied. Optimization energy tolerances of 2.0×10^{-5} hartree were used, but no vibrational analysis was performed. DFT is expedient for clusters of this size and has been extensively validated.^{33–37} The starting geometry was based on the X-ray crystal structure coordinates of diphenyldiselenoarsinic acid $[(\text{Ph})_2\text{AsSe}_2]^-$ and was generated by replacement of phenyl groups with methyl groups.³⁸

Results and Discussion

Although inorganic arsenic (arsenite and arsenate) is a well-established human carcinogen³⁹ and even though its mammalian metabolism has been extensively studied,⁴⁰ strikingly little is known about the molecular form(s) of arsenic inside cells. It is therefore not surprising that the mechanism of arsenite-induced carcinogenesis in humans is not completely understood.⁴¹ One way to gain insight into the molecular mechanism(s) is to characterize the arsenite metabolites that are formed in vivo. Subsequent toxicological evaluation of these metabolites could then reveal the actual carcinogenic species.

Arsenite, which exists at pH 7.4 as neutral arsenous acid $[\text{As}(\text{OH})_3]$, has a high chemical affinity for thiols and reacts with GSH under physiological conditions to give $(\text{GS})_3\text{As}$.^{42,43} Conversely, dimethylarsinic acid is reduced by 2 mol equiv of GSH to dimethylarsinous acid which reacts with one more GSH to yield *S*-(dimethylarsino)glutathione.⁴⁴ The biochemistry of selenite is also largely determined by its interactions with thiols, but in contrast to arsenite, selenite undergoes a redox reaction with 4 mol equiv of GSH to give GS-Se-SG and GSSG .¹¹ In vivo GS-Se-SG is further reduced to HSe^- (by glutathione reductase and NADPH),¹¹ which is then used either for the synthesis of methylselenium compounds¹¹ or for the formation of monoselenophosphate⁴⁵ which is then used for selenoprotein biosynthesis.⁴⁶

The discovery of a striking mutual detoxification between arsenite and selenite in mammals,^{14,15} however, indicated that the metabolism of arsenite is fundamentally intertwined with that of selenite. The lack of appropriate physicochemical techniques to structurally characterize a potential detoxification compound at the time, however, severely hampered the elucidation of the molecular mechanism. Using XAS and SEC-ICP-AES, a previously unknown As-, Se-, and S-containing detoxification species was recently detected in vivo and identified as $[(\text{GS})_2\text{AsSe}]^-$.^{18–20} Subsequent work showed that this species can be formed by nucleophilic attack of HSe^- on the arsenic atom of $(\text{GS})_2\text{As-OH}$ followed by displacement of the OH group.⁴⁷ Furthermore, the in vivo formation of $[(\text{GS})_2\text{AsSe}]^-$ suggests that the involved arsenic–selenium bonds are stronger than the hydrolytically unstable arsenic–sulfur bonds.⁴³ Consequently, the biochemistry of arsenite is driven not only by its interaction with thiols, but also by its interaction with intracellularly generated, highly reactive selenium metabolites, such as HSe^- . Accordingly, other arsenic compounds may react in a similar

(26) George, M. J. *J. Synchrotron Radiat.* **2000**, *7*, 283–287.

(27) <http://www-ssrl.slac.stanford.edu/exafspak.html>.

(28) Rehr, J. J.; Mustre de Leon, J.; Zabinsky, S. I.; Albers, R. C. *J. Am. Chem. Soc.* **1991**, *113*, 5135–5140.

(29) Delley, B. *J. Chem. Phys.* **1990**, *92*, 508–517.

(30) Delley, B. *J. Chem. Phys.* **2000**, *113*, 7756–7764.

(31) Becke, A. D. *J. Chem. Phys.* **1988**, *88*, 2547–2553.

(32) Perdew, J. P.; Wang, Y. *Phys. Rev. B* **1995**, *45*, 13244–13249.

(33) Ziegler, T. *Chem. Rev.* **1991**, *91*, 651–667.

(34) Fan, L.; Ziegler, T. *Density Functional Theory of Molecules, Clusters and Solids*; Ellis, D. E., Ed.; Kluwer: Dordrecht, The Netherlands, 1995; pp 67–95.

(35) Scheiner, A. C.; Baker, J.; Andzelm, J. W. *J. Comput. Chem.* **1997**, *18*, 775–795.

(36) Curtiss, L. A.; Raghavachari, K.; Redfern, P. C.; Pople, J. A. *J. Chem. Phys.* **1997**, *106*, 1063–1079.

(37) Delley, B. *Modern Density Functional Theory: A Tool for Chemistry*; Seminario, J. M., Politzer, P. P., Eds.; Elsevier: Amsterdam, 1995; Vol. 2, pp 221–254.

(38) Kanda, T.; Mizoguchi, K.; Kagohashi, S.; Kato, S. *Organometallics* **1998**, *17*, 1487–1491.

(39) Wang, Z.; Rossman, T. G. *Toxicology of Metals*; Chang, L. W., Ed.; CRC Lewis Publishers: Boca Raton, FL, 1996; pp 221–229.

(40) Aposhian, H. V. *Annu. Rev. Pharmacol. Toxicol.* **1997**, *37*, 397–419.

(41) Goering, P. L.; Aposhian, H. V.; Mass, M. J.; Cebrian, M.; Beck, B. D.; Waalkes, M. P. *Toxicol. Sci.* **1999**, *49*, 5–14.

(42) Scott, N.; Hatlelid, K. M.; MacKenzie, N. E.; Carter, D. E. *Chem. Res. Toxicol.* **1993**, *6*, 102–106.

(43) Gailer, J.; Lindner, W. *J. Chromatogr., B* **1998**, *716*, 83–93.

(44) Cullen, W. R.; McBride, B. C.; Reglinski, J. *J. Inorg. Biochem.* **1984**, *21*, 179–194.

(45) Glass, R. S.; Singh, W. P.; Jung, W.; Veres, Z.; Scholz, T. D.; Stadtman, T. C. *Biochemistry* **1993**, *32*, 12555–12559.

(46) Burk, R. F.; Hill, K. E. *BioEssays* **1999**, *21*, 231–237.

(47) Gailer, J.; George, G. N.; Pickering, I. J.; Buttigieg, G. A.; Denton, M. B.; Glass, R. S. *J. Organomet. Chem.* **2002**, *650*, 108–113.

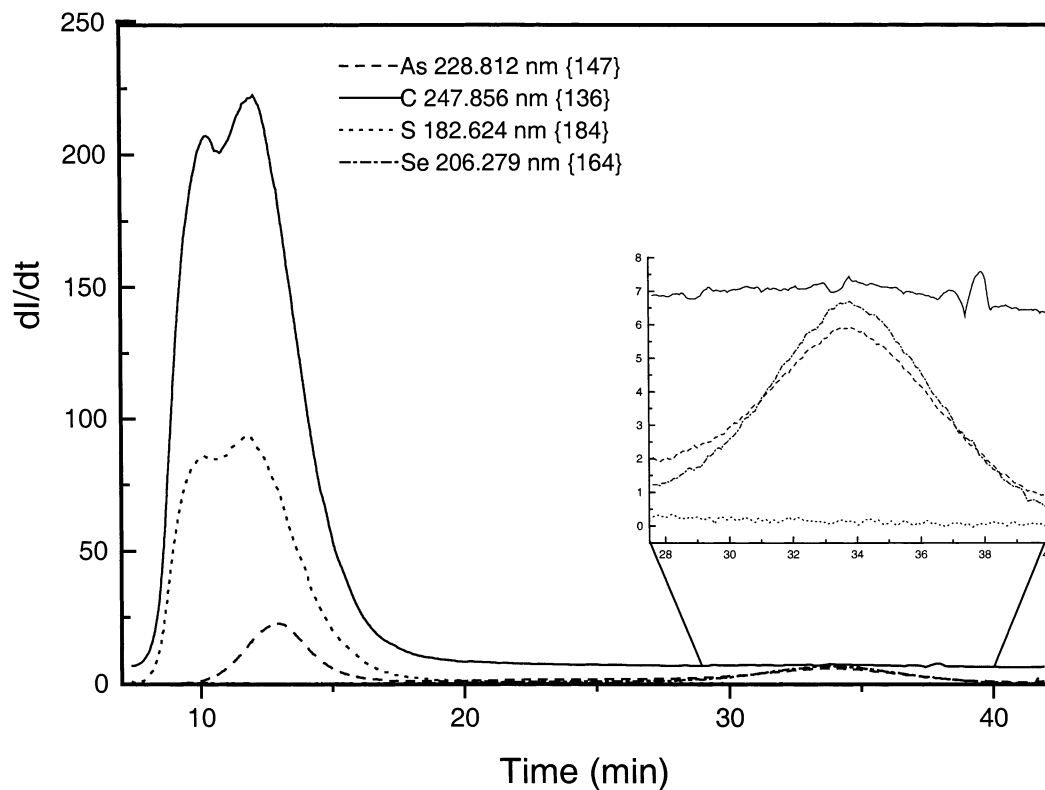


Figure 1. Size-exclusion chromatogram of the reaction product using arsenic-, sulfur-, selenium-, and carbon-specific detection by ICP-AES at 228.812 nm (order 147), 182.624 nm (order 184), 206.279 nm (order 164), and 247.856 nm (order 136), respectively.

fashion. In fact, selenite inhibited the induction of tetraploidy by dimethylarsinic acid⁴⁸ and dimethylarsinic acid also plays a role in the carcinogenesis of inorganic arsenic.⁴⁹ Therefore, a systematic investigation of the reaction between dimethylarsenic acid, selenite, and GSH was undertaken.

The reaction of excess GSH with equimolar selenite and dimethylarsinic acid yielded a colorless solution that showed a single ⁷⁷Se NMR resonance at 112.8 ppm (see Supporting Information). Since unreacted selenite would display a resonance of approximately 1300 ppm,²⁵ this finding implied the formation of an arsenic–selenium species with a single type of selenium atoms.

Analysis of this mixture by SEC-ICP-AES using simultaneous four-element-specific detection of As, Se, S, and C resulted in the chromatogram shown in Figure 1. The sulfur- and carbon-specific chromatogram contained two unresolved peaks with retention times of 10.1 and 12.1 min (Figure 1), compared with 9.0 and 11.6 min for GSSG and GSH standards, respectively. Although the retention times of the standards do not exactly match the retention times of the observed peaks (possibly due to matrix effects), the first sulfur/carbon peak is tentatively identified as GSSG, since redox chemistry seems likely, and since GSSG was also formed in a similar redox reaction involving selenite and GSH.^{18,50} The arsenic-specific chromatogram revealed the

elution of 54% of the injected arsenic in a peak with a retention time of 13.0 min and the balance in a second peak at 34.0 min (Figure 1). Since the first arsenic peak coeluted with a sulfur/carbon peak, we tentatively identify this peak as an arsenite–GSH species. The selenium-specific chromatogram showed only one peak with a retention time of 34.0 min which coeluted with the second arsenic peak and did not contain sulfur (Figure 1, inset). Although the carbon-specific chromatogram was very noisy, the presence of carbon in this arsenic–selenium species is indicated by the slightly increased emission at the peak maximum compared to the beginning and the end of the peak (Figure 1, inset). The As:Se intensity ratio revealed an As:Se molar ratio of 1:2, which is consistent with the observation that approximately half of the injected arsenic eluted in this peak (equimolar selenite and dimethylarsinic acid were reacted).

Substitution of the mobile phase with distilled water still yielded adequate separation of the arsenic–selenium species from the preceding sulfur- and carbon-containing peak, and allowed the collection of this peak (from 15 to 16.6 min) for subsequent ESI-MS analysis (Figure 2). The ESI-MS spectrum in the negative ion mode showed peaks (m/z 258–269) that were consistent with a formula of $\text{C}_2\text{H}_6\text{AsSe}_2$ (Figure 2, inset a, theoretical isotope distribution). The ion with the highest intensity at m/z 264.9 was then selected and collided with He at 27% relative energy in the Finnigan LCQ ion trap mass spectrometer. The selected ion fragmented via two main pathways: (1) loss of CH_3 (leading to m/z 249.7) and (2) loss of $(\text{CH}_3)_2\text{As}$ (leading to m/z 159.9). Thus, the ESI-MS-MS fragmentation spectrum (Figure 2, inset b)

(48) Ueda, H.; Kuroda, K.; Endo, G. *Anticancer Res.* **1997**, *17*, 1939–1944.

(49) Kenyon, E. M.; Hughes, M. F. *Toxicology* **2001**, *160*, 227–236.

(50) Gailer, J.; George, G. N.; Pickering, I. J.; Madden, S.; Prince, R. C.; Yu, E.; Denton, M. B.; Younis, H. S.; Aposhian, H. V. *Chem. Res. Toxicol.* **2000**, *13*, 1135–1142.

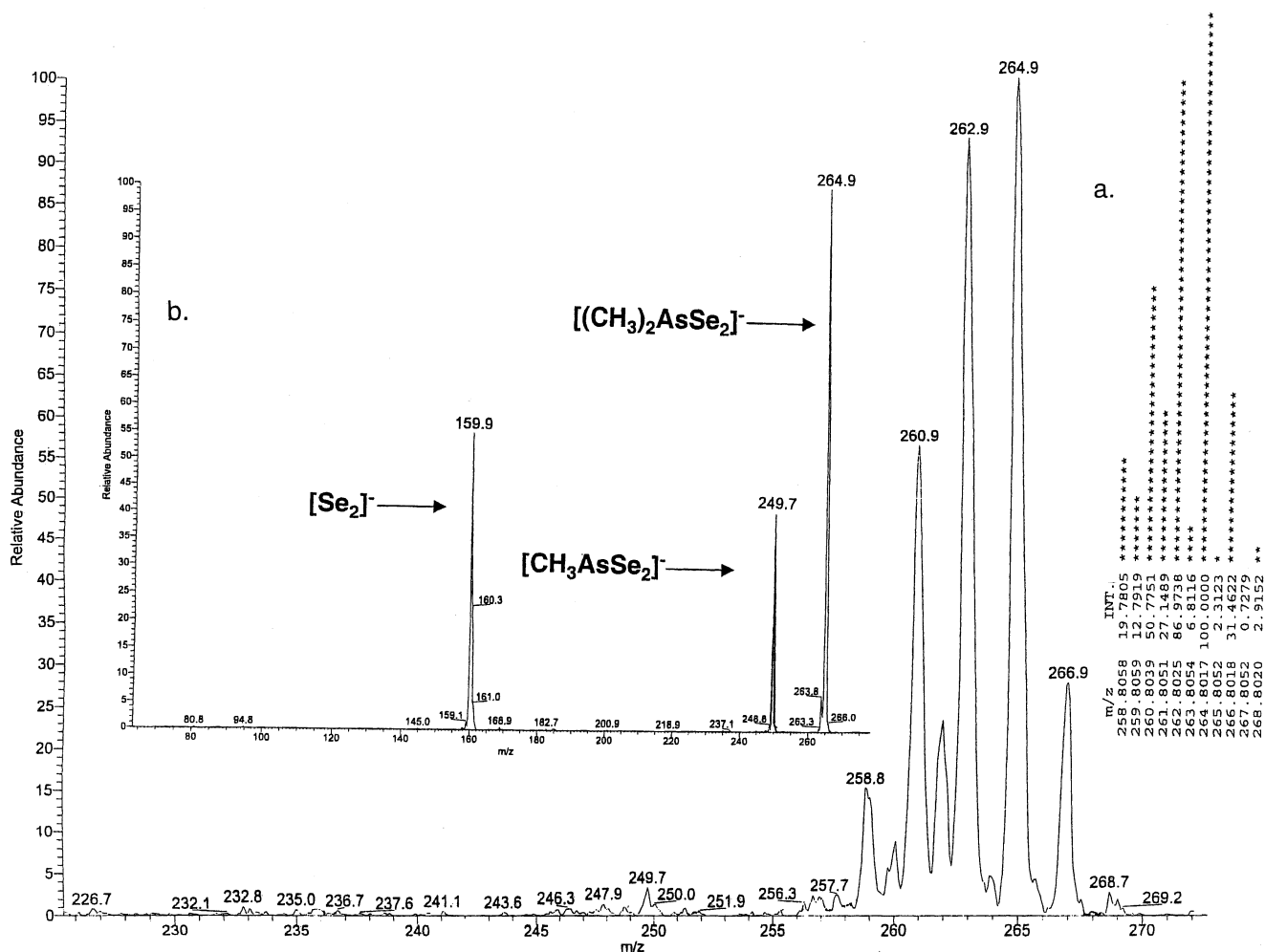


Figure 2. ESI-MS in the negative ion mode. Inset a: theoretical isotope distribution. Inset b: ESI-MS-MS fragmentation spectrum of the parent ion at m/z 264.9.

together with the SEC-ICP-AES results suggested the structure of the arsenic–selenium solution species to be $[(\text{CH}_3)_2\text{AsSe}_2]^-$. In corroboration of this, the structurally closely related species $[\text{Ph}_2\text{AsSe}_2]^-$ gave a ^{77}Se NMR shift of between 26.4 and 41.9 ppm (depending on the temperature),³⁸ compared with 112.8 ppm for the species reported in this study. These values are in good accord given that the ^{77}Se NMR spectra were recorded under different conditions and that ^{77}Se NMR chemical shifts are typically dependent on temperature, solvent, and pH.²⁵ Although the synthesis of the sodium salt of $[(\text{CH}_3)_2\text{AsSe}_2]^-$ from sodium cacodylate and H_2Se in ethanol has been previously briefly described,⁵¹ a full structural analysis of this compound was not reported.

The As and Se K near-edge X-ray absorption spectra of the purified synthetic arsenic–selenium solution species are shown in Figure 3 and clearly indicate the presence of a trivalent As species when compared to other near-edge spectra (Figure 3).¹⁸ In addition, the shape of the Se K near edge of the synthetic arsenic–selenium species is very similar to that previously reported for $[(\text{GS})_2\text{AsSe}]^-$, suggesting the presence of a somewhat similar electronic structure around the selenium atom (Figure 3).¹⁸ The arsenic and selenium

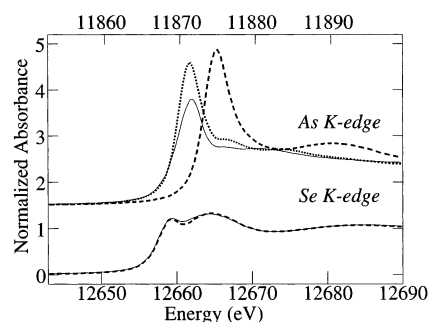


Figure 3. Arsenic and selenium near-edge X-ray absorption spectra of the purified arsenic–selenium reaction product (solid lines), arsenite (···, top), arsenate (---, top), and $[(\text{GS})_2\text{AsSe}]^-$ (---, bottom). The arsenic and selenium spectra are shown at the top and bottom of the plot, respectively, and their abscissas at the upper and lower edges of the plot.

K-edge extended X-ray absorption fine structure spectra of the purified synthetic arsenic–selenium solution species (Figure 4) confirmed the structure suggested by the ESI-MS-MS, ^{77}Se NMR, and the SEC-ICP-AES data. The As K-edge EXAFS (Figure 4), which is necessarily truncated at $k = 13.5 \text{ \AA}^{-1}$ by the Se K edge, gives a single broad Fourier transform peak, and is well fitted by two As–C at 1.92 Å and two As–Se at 2.27 Å. Both of these interactions are required for an adequate fit to the data. The Se K-edge

(51) Kuchen, W.; Förster, M.; Hertel, H.; Höhn, B. *Chem. Ber.* **1972**, *105*, 3310–3316.

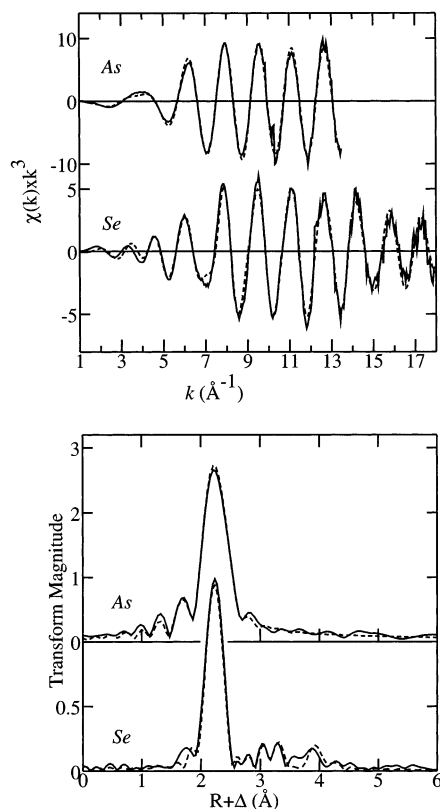


Figure 4. As and Se EXAFS (top) and corresponding Fourier transforms (bottom) of the purified arsenic-selenium reaction product. Data are shown as a solid line, with the results of the best fits shown as a dashed line. The As EXAFS is truncated by the Se K edge. The Fourier transforms have been phase-corrected for the first-shell (As-Se or Se-As) interactions. Note that different ordinate scales are used for the different elements.

EXAFS is dominated by a single interaction which corresponds to one Se-As at a distance of 2.27 Å, which is identical to that determined from the arsenic EXAFS. Additionally, the Se EXAFS shows three weak outer shell interactions in the range 3–4 Å, which are well-modeled as the more distant Se···Se (one at 4.15 Å), Se···C (two at 3.5 Å) and Se···O (two at 3.35 Å). These distant oxygen atoms are assigned to water molecules hydrogen bonded to the negatively charged selenium atoms since similar interactions have been observed in the EXAFS of Br^- and R-Se^- species (data not shown).

Taken together, our data conclusively indicate the formation of the dimethyldiselenoarsinate anion, $[(\text{CH}_3)_2\text{AsSe}_2]^-$. Figure 5 shows the density functional theory computed structure of this ion (in a vacuum), which yielded As-Se and As-C distances of 2.32 and 1.99 Å, respectively, a Se···Se distance of 4.10 Å, and a Se···C distance of 3.48 Å. Given the well-known tendency of density functional methods to yield bond lengths that are slightly longer than reality, these are in excellent agreement with those determined by EXAFS.

Previously, the mechanism of formation of $[(\text{GS})_2\text{AsSe}]^-$ from selenite, arsenite, and GSH was shown to involve the nucleophilic attack of HSe^- on $(\text{GS})_2\text{As-OH}$,⁴⁷ and the formation of $[(\text{CH}_3)_2\text{AsSe}_2]^-$ (from selenite, dimethylarsinic acid, and GSH) most likely involves a similar reaction

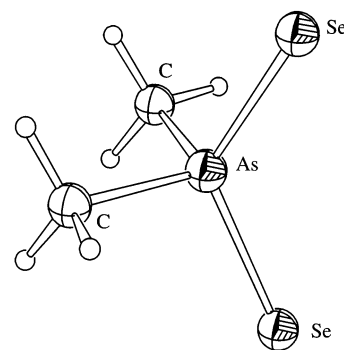


Figure 5. Calculated structure of $[(\text{CH}_3)_2\text{As}(\text{Se})_2]^-$ obtained with Dmol³ as discussed in the text.

Table 1. Coordination Numbers N , Interatomic Distances R (in Å), Debye-Waller Factors σ^2 (Mean-Square Deviations in Interatomic Distance, in Å²), and Threshold Energy Shifts ΔE_0 (in eV)^a

	N	R	σ^2	ΔE_0
As-C	2	1.923 (4)	0.0019 (3)	-9.2 (7)
As-Se	2	2.271 (2)	0.0024 (1)	
Se-As	1	2.271 (1)	0.0023 (1)	-16.7 (5)
Se···C ^b	2	3.502 (7)	0.0045 (9)	
Se···O ^b	2	3.345 (8)	0.0067 (8)	
Se···Se ^b	1	4.149 (7)	0.0063 (6)	

^a The values in parentheses are the estimated standard deviations obtained from the diagonal elements of the covariance matrix. Only single scattering terms were included in the fits reported; when multiple scattering terms were included these had amplitudes that were insignificant (less than 0.1% of the largest interaction). Se and As EXAFS were fitted independently, with values for S_0^2 assumed to be 1.0 (this was verified by fitting model compounds). ^b These components contribute in only a minor way to the fit, and their assignment is correspondingly tentative.

mechanism. Since $[(\text{CH}_3)_2\text{AsSe}_2]^-$ contains trivalent arsenic (Figure 3), dimethylarsinic acid was first reduced by 2 mol equiv of GSH to the trivalent arsenic species dimethylarsinous acid, as reported.^{44,52} Consecutive nucleophilic attack of two HSe^- molecules (formed from selenite and 6 mol equiv of GSH) on the arsenic atom followed by displacement of the OH group of dimethylarsinous acid most likely yields $[(\text{CH}_3)_2\text{AsSe}_2]^-$.

Conclusion

The reaction of equimolar dimethylarsinic acid and selenite with 10 mol equiv of GSH yielded a novel arsenic-selenium solution species. Structural elucidation of the reaction product by ⁷⁷Se NMR, SEC-ICP-AES, ESI-MS-MS, and arsenic and selenium EXAFS spectroscopy unequivocally revealed that the dimethyldiselenoarsinate anion, $[(\text{CH}_3)_2\text{AsSe}_2]^-$, had formed. Since another structurally related arsenic-selenium species, the seleno-bis (*S*-glutathionyl)arsinium ion, $[(\text{GS})_2\text{AsSe}]^-$, was previously detected in rabbit bile,^{18–20} and because dimethylarsinic acid is an environmentally abundant arsenic compound, further studies are necessary to investigate whether the $[(\text{CH}_3)_2\text{AsSe}_2]^-$ anion is formed in vivo.

Acknowledgment. This work was funded by the Alexander von Humboldt Foundation and Thermo Jarrel Ash

(52) Delnomdedieu, M.; Basti, M. M.; Otvos, J. D.; Thomas, D. J. *Chem.-Biol. Interact.* **1994**, *90*, 139–155.

Corporation (Franklin, MA). The Stanford Synchrotron Radiation Laboratory (SSRL) is a national user facility operated by Stanford University on behalf of the U.S. Department of Energy, Office of Basic Energy Sciences. The SSRL Structural Molecular Biology Program is supported by the Department of Energy, Office of Biological and Environmental Research, and by the National Institutes of

Health, National Center for Research Resources, Biomedical Technology Program.

Supporting Information Available: ^{77}Se NMR spectrum of $[(\text{CH}_3)_2\text{AsSe}_2]^-$ in D_2O . This material is available free of charge via the Internet at <http://pubs.acs.org>.

IC0113146